PCCP

Accepted Manuscript

ROYAL SOCIETY OF CHEMISTRY

www.rsc.org/pccp

Experimental and First-Principles Study of Guanine Adsorption on the ZnO Clusters

V.L. Chandraboss, B. Karthikeyan and S. Senthilvelan*

Department of Chemistry, Annamalai University, Annamalainagar 608 002

E-mail: dr_senthilvel@yahoo.co.in

*Address for correspondence

Dr. S. Senthilvelan
Assistant Professor,
Department of Chemistry,
Annamalai University,
Annamalai nagar-608 002,
Tamilnadu, India.
Tel.: +91 9486389270
E-mail: dr_senthilvel@yahoo.co.in

Experimental and First-Principles Study of Guanine Adsorption on the ZnO Clusters

V.L. Chandraboss, B. Karthikeyan and S. Senthilvelan*

Department of Chemistry, Annamalai University, Annamalainagar 608 002

E-mail: dr_senthilvel@yahoo.co.in

ABSTRACT

Theoretical investigation of guanine, a DNA base adsorption on the ZnO model clusters, viz., Zn_2O_2, Zn_3O_3, Zn_4O_4 ring (R) and Zn_4O_4 wurtzite (W) in terms of geometry, binding site, binding energy (E_B), energy gap (E_g), electronic and spectral properties were studied by density functional theory (DFT) method. Guanine adsorption on the ZnO (G/ZnO) clusters is modeled by B3LYP/LanL2DZ method. The calculated binding energy (E_B) and energy gap (E_g) of the molecule guanine is highly dependent on the nature of the cluster size and vary with the size of the clusters. Physisorption proceeded via the formation of N...Zn bond between the guanine and active Zn^{2+} site on ZnO is proposed. The HOMO-LUMO energies show that charge transfer occurs in the G/ZnO clusters, from ZnO to guanine to better understand the interaction. The Mulliken charges are computed. The electronic properties of ZnO and G/ZnO clusters has been compared with different basis sets (B3LYP/6-31G, B3LYP/6-311G, MP2/6-31G and MP2/LanL2DZ). Experimental information like microscopic and spectroscopic evidence is also included to understand the guanine-ZnO interactions. G/ZnO composite was prepared by precipitation method and it was characterized by SEM with EDX, FT-IR and FT-RAMAN analysis. The interaction of guanine with ZnO nanoparticles were observed by UV-vis spectroscopy. Experimental results are compared with the DFT results in the light of these new insights.

1. INTRODUCTION

The application of nanotechnology in medical applications, commonly referred as "Nanomedicine", delivers a set of tools, devices and therapies for the treatment of human disease.[1-3] Nanoparticles of ultra small size are comparable to the naturally occurring proteins and biomolecules in the cell. These nanoparticles can alter their structural, morphological, electrical, magnetic and chemical properties enabling them to interact in unique ways with the cell biomolecules and enable their physical transport into the interior structure of the cells.[4] ZnO nanoparticles can adequately be considered as an ideal candidate for biomedical applications by virtue of their nontoxic nature, low cost, biosafty and biocompatible and its wide usage in the daily life, such as drug carriers and cosmetics.[5-10] ZnO nanoparticles in biomedical and cancer applications are gaining interest in the scientific and medical communities, largely due to the physical and chemical properties of these nanomaterials.[11] ZnO nanoparticles can kill cancer and activated human T cells, suggesting biotherapeutic functionality of this novel material.[12]

The photoactive surfaces of the nanoparticles produce reactive oxygen species (ROS) that can potentially cause oxidative stress that leads to cellular protein, lipid and DNA damage.[13-15] But, one promising biocompatible and nontoxic semiconductor material is ZnO,[16] which has found widespread application as a UV-blocker for skin protection gels and creams.[17,18] The small size of the ZnO nanoparticles reduces the "scattering" of visible light and providing "transparent" products which retain UV absorption.[19] There is no evidence that ZnO nanoparticles possess a photo-toxic or photo-genotoxic risk to humans. One has to consider that there is robust evidence that this substance protects human skin against UV-induced adverse effects, including skin cancer and DNA damage.[19]

Inorganic nanostructures (nanowires, nanotubes, nanofibers and quantum dots) interacting with biological molecules (adenine, guanine, cytosine, thymine and uracil) to produce novel hybrid materials is important for future advancements in biomedical nanotechnology.[20-24] The combination of ZnO with biomolecule is of particularly intriguing since it opens the door to novel bio and nanotechnological applications.[25] ZnO prefers to bind with a ring nitrogen atom (N-site) having a lone electron pair relative to other possible binding sites of the DNA bases. In most of the cases adsorption and interaction strength of ZnO with N-site of the guanine is much higher than other sites.[25]

One of the major thrusts in the study of clusters is to develop fundamental understanding of materials at the nanoscale as the properties and structures are often quite different from bulk and depend on size and shape as well.[26] To realize such application a detailed understanding of the fundamental molecular interactions and physical properties of the composite is required. While it is becoming possible to investigate clusters and biomolecule interaction along with its experimental information, the present status, therefore, requires a more detailed knowledge of the nanometal oxide-biomolecule interactions at the fundamental level. Full scale quantum mechanical calculations consisting of DNA strands are prohibitively expensive. So, guanine (2-amino-1,7-dihydro-6H-purin-6-one, $C_5H_5N_5O$), an important DNA base has been chosen for this study. This base is often involved in bio processes such as mutations leading to carcinogenesis and is one of the main targets of anticancer drugs, namely, cisplatin and its analogues.[27-29] So, in the present work we have performed a detailed first principles quantum chemical study of guanine and its interaction with different ZnO clusters.

We focus our attention on adsorption of guanine with a ZnO clusters in terms of energy, geometry, binding site, electronic properties, HOMO-LUMO charge distribution plots and Mulliken charges have been also performed. A simulated IR and RAMAN spectra of ZnO and G/ZnO clusters (DFT level) were studied and compared with experimental data. G/ZnO composite was characterized by surface morphology and spectroscopy analysis. UV-visible absorption studies are most applicable in G/ZnO composite. This work aims to contribute to the investigation of weak interaction between guanine and ZnO clusters at preferred N1-site of the guanine. Experimental and theoretical information favored physisorption, the formation of weak Zn-N bond in G/ZnO models. The electronic properties favored to form the most stable G/Zn_2O_2 cluster and the reduction of energy gap value of ZnO, after adsorption of guanine on the ZnO clusters.

2. EXPERIMENTAL SECTION

2.1. Materials

Zinc acetate dihydrate ($Zn(CH_3COO)_2 \cdot 2H_2O$), oxalic acid ($C_2H_6O_6$), anhydrous ethanol ($C_2H_5OH$) and guanine ($C_5H_5N_5O$) were the guaranteed reagents of Sigma Aldrich and used as such. All glassware's were cleaned with chromic acid followed by thorough washing with distilled water.

2.2. Preparation of guanine adsorption on the ZnO nanoparticles (G/ZnO composite)

Zinc acetate dihydrate (0.8 M) was dissolved in anhydrous ethanol. The precursor solution was added dropwise into oxalic acid with ethanol solution at room temperature under vigorous stirring until a precipitate formed. The obtained precipitate was washed with water and ethanol. Then the precipitate was collected and dried in oven at 100 ^oC for 12 h in air. The resulting material was calcined at 500 ^oC for 2 h, to obtain ZnO nanoparticles. The ZnO

nanoparticles and guanine molecule were dispersed in 50 mL conductivity water. The mixture was sonicated for 30 mins and filtered. The obtained precipitate was dried at 100 ^{o}C for 5 h. To obtained final material was ground well to get a G/ZnO composite. This G/ZnO composite was characterized by SEM with EDX, FT-IR and FT-RAMAN analysis.

2.3. Computational Details

The optimized geometry of the ZnO clusters and the interaction of guanine with ZnO clusters have been studied by density functional theory (DFT) method at B3LYP/ LanL2DZ levels of theory, using the Gaussian 03W package of program.[30] In this work ZnO and G/ZnO clusters electronic properties are compared by different basis sets (B3LYP/6-31G, B3LYP/ 6-311G, MP2/6-31G and MP2/LanL2DZ). Molecular structure was visualized with Chemcraft 1.6 software. In order to obtain a density of state (DOS) curves, output was analyzed using Gausssum[31] programs. For the Zn atoms, the standard LanL2DZ basis set was used.[32] The B3LYP functional yields reasonable results for small clusters in earlier studies and has been reliable for predicting energy gap values for a variety of metal oxides.[32-34]

2.4. Characterization methods

Fourier transform-infrared spectra (FT-IR) were recorded using SHIMADZU FT-IR spectrometer in KBr pellet. Fourier transform-Raman (FT-Raman) spectra were recorded with an integral microscope Raman system RFS27 equipped with 1024 X 256 pixels having liquefied nitrogen-cooled germanium detector. The 1064 nm line of the Nd:YAG laser (red laser) was used to excite. To avoid intense heating of the sample, the laser power at the sample was maintained as 15 mW. Each spectrum was recorded with an acquisition time of 18 sec. Scanning electron microscopy (SEM) with elementary dispersive X-ray analysis (EDX) experiments were carried out at 25 °C on an FEI Quanta FEG 200 instrument with EDX analyzer facility.

The sample was prepared by placing a small quantity of the prepared material on a carbon coated copper grid and allowing the solvent to evaporate. UV-vis (ultraviolet and visible light) absorbance spectra were measured over a range of 600-200 nm with a Shimadzu UV-1650PC recording spectrometer using a quartz cell with 10 mm of optical path length.

RESULTS AND DISCUSSION

3.1. Optimized structure of ZnO clusters

The optimized structures of ZnO clusters, such as Zn_2O_2, Zn_3O_3, Zn_4O_4 (R) and Zn_4O_4 (W) were shown in Fig. 1. The details of the clusters, scaled energies, HOMO–LUMO energy gab and binding energies were given in Table. 1. Scaled energies are used throughout the study to allow a direct comparison between the energies of ZnO clusters with different sizes.[31] Total energies scaled with the cluster size are also included in the Table. 1.

The scaled energy $E_S = E/N$, where E is the total energy and N is the number of atoms in the cluster. The binding energy of ZnO clusters were calculated by $E_B = [(nE_{Zn}+nE_O–E_{(ZnO)})/n]$, where n is the number of ZnO molecules in the cluster. The bond lengths of ZnO clusters $R_{(Zn–O)}$ is in the range of 1.82–1.99 Å. The Zn–O bond is mainly ionic with a charge transfer from Zn to O atoms. The energy gap ($E_g = E_{LUMO} − E_{HOMO}$) of the ZnO clusters were calculated from the total densities of states (DOS). As shown in Fig. 2, the E_g value of Zn_2O_2, Zn_3O_3, Zn_4O_4 (R) and Zn_4O_4 (W) is 2.30 eV, 3.74 eV 3.90 eV and 2.25 eV. As shown in Table. 1, the E_B value of Zn_2O_2, Zn_3O_3, Zn_4O_4 (R) and Zn_4O_4 (W) is 6.12 eV, 7.34 eV, 7.75 eV and 7.21 eV. The binding energy and energy gap value of Zn_4O_4 (R) is higher when compared to Zn_2O_2, Zn_3O_3 and Zn_4O_4 (W) clusters were concluded. Zn_4O_4 (R) is a more stable structure favors the larger HOMO-LUMO gap and more binding energy.

3.2. Optimized structure of guanine adsorption of the ZnO clusters (G/ZnO models)

The optimized structures of guanine adsorption on the ZnO clusters (G/ZnO models) were shown in Fig. 3. ZnO cluster is considered approaching the guanine toward the most favored five membered ring (–N1 site) of the guanine molecule. The details and computed properties of the G/ZnO clusters were also given in Table. 1. The clusters containing Zn and O atoms [Zn_2O_2, Zn_3O_3, Zn_4O_4(R) and Zn_4O_4 (W)] were used to investigate the interaction between guanine molecule and ZnO. Guanine is a bicyclic molecule comprising a fused pyrimidine (*Pyr*)-imidazole (*Im*) ring system. Optimized structure and DOS spectrum of guanine is shown in Fig. 4. To better understand the interaction between guanine with the ZnO clusters, the influence of guanine adsorption on the electronic properties of the clusters was taken into account.

Thus we have calculated the corresponding binding energies as $E_B = [E_{Total(G/ZnO)} - (E_{ZnO} + E_G)]$, where $E_{Total(G/ZnO)}$ is the total energy of guanine adsorbed on the ZnO clusters. E_{ZnO} and E_G are the total energies of the individual ZnO clusters and guanine respectively. From the optimized structure and binding energy values it was seen that in all cases, ZnO clusters prefers to bind through the ring nitrogen atom of guanine depending on the surface nature of ZnO clusters. When guanine attached through ring nitrogen sites on the ZnO surface an overlap occurs between Zn–d and N–P orbital that leads to a greater binding energy for the ring N1 site.[4]

The calculated nearest-neighbor distance (R) in the equilibrium configurations associated with the binding sites generally reflect the predicted order of the bonding energy,[25] $R_{Zn-N(ring)}$ is reported in the range of 2.04–2.08 Å. The Zn–N bond distance in the case of G/Zn_2O_2 is shorter (2.04 Å) when compared to G/Zn_3O_3 (2.06 Å), G/Zn_4O_4 (W) (2.07 Å) and G/Zn_4O_4 (R) (2.08 Å) models. This also further clear from the binding energy of G/Zn_2O_2 (2.17 eV) is higher when compared to G/Zn_3O_3 (1.90 eV), G/Zn_4O_4 (W) (1.63 eV) and G/Zn_4O_4 (R) (1.62eV)

models. The order for the binding energy and bond distance from G/ZnO models on the preferred N1-site is G/Zn_2O_2 > G/Zn_3O_3 > G/Zn_4O_4 (W) > G/Zn_4O_4(R). The preferred G/Zn_2O_2 model is most favor compared to other G/ZnO clusters. The binding energy and bond distance of G/Zn_4O_4 (W) is more favorable compared to G/Zn_4O_4 (R). Therefore, be concluded that the covalent forces play the key role in deciding the strength of interaction. The nearest-neighbor distance confirms the interaction regime for covalent forces.[25,35]

The difference in energy between the HOMO and LUMO was calculated from the DOS results (Fig. 5). As shown in Table 1, the Eg of guanine adsorption on Zn_2O_2, Zn_3O_3, Zn_4O_4 (R) and Zn_4O_4 (W) clusters are 2.81 eV, 3.92 eV, 4.0 eV and 2.34 eV. On the basis of our calculations, guanine on the ZnO clusters induces some changes in the electronic properties of ZnO clusters and the E_g value are slightly increased after adsorption process, as shown in Figs. 2 and 5, with comparison of DOS of the ZnO clusters and G/ZnO models. It is found that the E_g value of ZnO clusters have been increased about 0.51 eV [Zn_2O_2], 0.18 eV [Zn_3O_3], 0.10 eV [Zn_4O_4 (R)] and 0.09 eV [Zn_4O_4 (W)] after the guanine adsorption on ZnO clusters. The order of changes occurs in the E_g values are Zn_2O_2 > Zn_3O_3 > Zn_4O_4 (R) > Zn_4O_4 (W). Also, more efficient binding have been achieved in Zn_2O_2 model. The E_g of guanine (4.85 eV) is slightly reduced, after adsorption on the ZnO clusters. The achieved reduction is 42% [G/Zn_2O_2], 19.1% [G/Zn_3O_3], 17.5% [G/Zn_4O_4 (R)] and 51.7% [G/Zn_4O_4 (W)].

The HOMO-LUMO analysis explains the charge transfer taking place within the G/ZnO clusters. Determination of the energies of the HOMO and LUMO are important parameters in quantum chemical calculations.[36] The HOMO is the orbital that primarily acts as an electron donor and the LUMO is the orbital that largely acts as the electron acceptor. Fig. 6. Shows the HOMO-LUMO electron distribution plots for G/Zn_2O_2, G/Zn_3O_3, G/Zn_4O_4 (R) and G/Zn_4O_4 (W)

clusters. In this energy level plot, the positive phase is shown in red and the negative one is green color. It can be seen from the 3D plots that the HOMO levels are spread over the entire ZnO clusters. The LUMO of first excited state is almost uniformly distributed over the guanine of G/Zn_3O_3 and G/Zn_4O_4 (R) clusters, except G/Zn_2O_2 and G/Zn_4O_4 (R). From our theoretical data the HOMO-LUMO energy gap values of G/Zn_2O_2 and G/Zn_4O_4 (R) is 2.04 and 2.07 eV, when compared to G/Zn_3O_3 and G/Zn_4O_4 (R) clusters (3.92 and 4.01 eV). Usually the clusters with larger HOMO-LUMO gaps are more stable and chemically inert.[37] The above observation show the charge transfer occurs in the G/Zn_3O_3 and G/Zn_4O_4 (R) clusters.

Mulliken charge distributions were calculated by determining the electron population of each atom as defined by the basis set.[38] The calculated Mulliken charge values using B3LYP/LanL2DZ levels of theory. Mulliken atomic charges of ZnO and G/ZnO clusters were given in Table. 2. For ZnO clusters Oxygen atoms exhibit a negative charge, which are donor atoms. Zn atoms exhibit a positive charge, which is an acceptor atom for ZnO clusters (Zn_2O_2, Zn_3O_3 and Zn_4O_4). From the G/Zn_4O_4 clusters N_1, C_2, N_3, N_5, N_7, N_8, O_{10}, O_{13}, O_{14}, O_{16} and O_{17} atoms exhibit a substantial negative charge (Except C_4, C_6, C_9, C_{11}), which are donor atoms. Zn_{12}, Zn_{15} and Zn_{18} atoms exhibits a positive charge, which is an acceptor atom. In all Hydrogen atoms have positive charges. The Zn_{12} (0.979) atom exhibit more positive charge and N_3 atom exhibit more negative charge (-0.346), these two atoms favor the weak interaction of Zn–N bond in G/ZnO clusters.

Zn_2O_2 is consider to approach the guanine toward other possible binding sites six membered ring (–N2 site), $–NH_2$ site and oxygen site (O site) of the guanine molecule. These possible binding sites for guanine are shown in Fig. 7. The calculated bond distance (Å), binding energy (E_B) and electronic properties of G/Zn_2O_2 (–N2, $–NH_2$ and –O) sites were

discussed. The Zn–N bond distance of –N2 and $–NH_2$ site is 2.06 Å and 2.14 Å. The Zn–O bond distance of –O site is 1.99 Å. The calculated binding energy of –N2, $–NH_2$ and –O sites are 1.71 eV, 1.61 eV and 3.30 eV. The HOMO-LUMO energy gap (E_g) value of G/Zn_2O_2 cluster is 0.71 eV (–N2 site), 1.40 eV ($–NH_2$ site) and 0.69 eV (–O site) respectively. The binding energy, bond distance and energy gap values favor the –O site of G/Zn_2O_2 cluster.

The energy gap (E_g) values of ZnO and G/ZnO clusters at different basis set (B3LYP/ 6-31G, B3LYP/6-311G, MP2/6-31G and MP2/LanL2DZ) have been shown in Table. 3. The E_g value increases with increasing size of ZnO clusters (Zn_4O_4 (R) > Zn_3O_3 > Zn_2O_2) in all basis sets, except Zn_4O_4 (W) which is a wurtzite type cluster. The E_g of G/ZnO clusters are also increases with increasing the size of the clusters. The basis sets MP2/6-31G, MP2/LanL2DZ, B3LYP/6-31G [except, G/Zn_2O_2 and G/Zn_4O_4 (W)] and B3LYP/6-311G [except, G/Zn_2O_2 and G/Zn_4O_4 (W)] favors the reduction of energy gap value of ZnO after adsorption of guanine on the ZnO clusters.

3.3. FT-IR analysis

The FT-IR spectra of the ZnO and G/ZnO composite are shown in Fig. 8. Transmittance is the main characteristic of Zn–O vibration[39] it depends mainly on the morphology of the ZnO nanoparticles. The IR spectrum (Fig. 8a) show the absorption peaks at 438, 539 and 1629 cm^{-1} is corresponds to Zn–O stretching vibration.[40] This metal-oxygen frequencies observed for the respective metal oxides are in accordance with the literature values.[41] From Fig. 8b, we can observe several peaks in the spectral range 1000−1800 cm^{-1} corresponding to C=C, C−C, C=O and N-H vibrations. The absorption bands at around 537 and 1580 cm^{-1} which were assigned to Zn–N bonding respectively.[42,43] Absorption peaks between the 2800-3050 cm^{-1} are due to C–H

stretching vibration of the alkane groups. We can also identify a broad resonance corresponding to OH group vibrations at ~3100−3600 cm^{-1}.

The simulated IR spectra of ZnO and G/ZnO clusters are presented in Fig. 9. For Zn_2O_2, Zn_3O_3 and Zn_4O_4 (R), the dominant peak of IR spectra shift from 550 cm^{-1} [Zn_2O_2] to 750 cm^{-1} [Zn_4O_4 (R)], while it comes back to 480 cm^{-1} for wurtzite structure of Zn_4O_4. For comparison the computed vibrational frequency of Zn_4O_4 cluster is 436 cm^{-1} and the experimental values for the ZnO nanoparticle is 438 cm^{-1} for E_{2H} mode respectively.[37] For G/ZnO clusters the absorption peaks between 40-200 cm^{-1} and 700-750 cm^{-1} are due to Zn–N stretching vibration. The absorption peaks between 1500-2000 cm^{-1}corresponding to C=C, C−C, C=O and N-H vibrations. For comparison the computed vibrational frequency of G/ZnO clusters of most intense peak 536 cm^{-1} and the experimental values for the G/ZnO composite is 537 cm^{-1}(Zn–N bond) respectively.[42]

3.4. FT-RAMAN analysis

FT-Raman spectra of ZnO and G/ZnO composite were shown in Fig. 10. ZnO belonging to C^4_{6v} space group has the following optic modes: A_1 +2B_1 + E_1 + 2E_2 at the point of the Brillouin zone, among which E_1, E_2, and A_1 are the first-order Raman-active modes, and B_1 is forbidden.[44] Meanwhile, the E_1 and A_1 modes split into longitudinal optical (LO) and transverse optical (TO) components. A_1, E_1 and E_2 mode are Raman-active. Two nonpolar Raman active modes are often assigned as E_2 (low), and E_2 (high). All these modes have been reported in the Raman scattering spectra of bulk ZnO.[45] The characteristic peaks at 212, 380, 438 and 569 cm^{-1}, which correspond to the 2TA; 2E_2(low), A_1(TO), E_2(high) and A_1(LO) fundamental phonon modes of ZnO, respectively. The Raman peak at 438 cm^{-1} is attributed to the ZnO nonpolar

optical phonons of high-E2 mode,[46] which is one of the characteristic peak of wurtzite ZnO (Fig. 10a).

Fig. 10b shows FT-Raman spectrum of G/ZnO composite. The corresponding Raman feature is at 397 cm^{-1} is also quite intense, which supports its assignment to the in-plane amino and carbonyl group deformations. The most intense feature in the Raman spectrum, observed at 648 cm^{-1} is ascribed to the in-plane/in-phase stretching of the purine ring. The C–H out-of-plane bending vibrations are strongly coupled vibrations and occur in the region 1000-750 cm^{-1}.[47] The spectral region above 1000 cm^{-1} contains mostly in-plane modes, all are Raman active. Guanine interacts with the ZnO surface through the lone pairs of nitrogen atoms. The weak 1046 cm^{-1} band results from contributions involving *Pyr*/*Im*N–C stretching modes.[48,49] The very weak peak at 721 cm^{-1}, which is related to a normal mode with prevailing contributions from the C=O and C–H out-of-plane bending modes.[50]

The simulated RAMAN spectra of ZnO and G/ZnO clusters are presented in Fig. 11. For Zn_2O_2, Zn_3O_3 and Zn_4O_4 (W) the most intense peak around 210-250 cm^{-1} and 438 cm^{-1} which is the main characteristic peaks at 212 and 438 cm^{-1} 2TA; $2E_2$(low) and E_2(high) fundamental phonon modes of ZnO nanoparticles.[44,45] For G/ZnO the spectral region between 1000-1800 cm^{-1} contains mostly in-plane modes, all are Raman active. The absorption peak around 569 corresponds to A_1(LO) fundamental phonon mode of ZnO, respectively. FT-IR and FT-RAMAN spectrum of guanine is shown in Figs. 8c and 10c. In our experimental data, FT-IR shows small spectral changes (1580 and 537 cm^{-1}) were observed in G/ZnO composite compared with guanine molecule. But, FT-RAMAN shows spectral changes in light. Therefore, experimental information is favored physisorption and the formation of weak bond in guanine-ZnO interactions. The results are also favored by DFT calculations.

3.5. SEM with EDX and FE-SEM analysis

SEM micrograph was used to examine the morphology and topography of the prepared materials. SEM micrograph shows the aggregated ZnO nanoparticles are almost spherical in shape and the average particle size is 85 nm (Fig. 12a). SEM image of G/ZnO composite (Fig. 12b) shows the particles are extensively agglomerated. EDX analysis confirms Zn and O are present in the ZnO material (Fig. 12c), Whereas Zn, O, C and N are present in G/ZnO composite material (Fig. 12d). The aggregated ZnO nanoparticle is ultra sonication for 40 mins at 50 °C, the aggregated nanoparticles are uniformly distributed and individual spherical nanoparticles were formed. The FE-SEM shows the individual spherical nanoparticles are almost 35 nm (Fig. 13a).

3.6. UV-vis spectroscopy

UV-vis absorption spectra of ZnO nanoparticles, G/ZnO composite and guanine molecule is shown in Fig. 13. We observed optical property of materials in deionized distilled water suspension. A broad band at 375 nm (3.30 eV) clearly indicates the existence of ZnO nanoparticles[40] (Fig. 13b). The absorption spectra of guanine exhibit two complex band systems. The low energy bands 246 and 271 nm is due to two electronic transitions with maxima at about 5.04 and 4.57eV. A broad band at 321 nm (3.86 eV) clearly observed in guanine molecule (Fig. 13c). The absorption spectrum of G/ZnO composite is shown in Fig. 13d. A broad band at 375 nm indicates ZnO nanoparticles. The strong and medium transitions observed at 246 and 274 nm are attributed to the $\pi-\pi^*$ transition while very weak absorption band determined at 321 nm corresponds to the $n-\pi^*$ transition.[36] The above observation energy gap of guanine is reduced after adsorption on ZnO nanoparticles. From our theoretical evidence also favored the reduction of E_g value of guanine is 51.7% [G/Zn_4O_4 (W) cluster].

4. CONCLUSIONS

We have investigated the electronic structure of guanine interacting with different sized ZnO clusters (Zn_2O_2, Zn_3O_3 and Zn_4O_4). We have identified ring N1-atom of guanine adsorbed and to form the most stable G/Zn_2O_2 cluster by DFT theory. The order for the binding energy, bond distance and energy gap values for guanine adsorbed ZnO clusters through the preferred N1-site is G/Zn_2O_2 > G/Zn_3O_3 > GZn_4O_4 (W) > G/Zn_4O_4 (R). The interaction between the guanine and ZnO clusters is dominated by the hybridization between Zn-d with N-p orbital that determines the interaction strength of guanine and ZnO with a marginal contribution from the ionic forces. On the basis of DFT calculations, it seems that adsorption of the guanine on the ZnO clusters induces some changes in the electronic properties of the ZnO clusters by using B3LYP/LanL2DZ. The HOMO-LUMO analysis confirms the charge transfer occurs. Mulliken charge distribution explains Zn_{12} (0.979) atom exhibit more positive charge and N_3 atom exhibit more negative charge (-0.346), these two atoms form the weak interaction of Zn–N bond in G/ZnO clusters. The calculation of MP2/6-31G, MP2/LanL2DZ, B3LYP/6-31G and B3LYP/ 6-311G favors the reduction of the energy gap value of ZnO, after adsorption of guanine on the ZnO clusters. UV-visible absorption studies most favored such weak interaction in G/ZnO composite. Our results find out the efficient binding could not be achieved by increasing the size of the clusters. SEM with EDX, FT-IR, FT-Raman and UV-vis absorption analysis shows adsorption of guanine on the ZnO surface having through physisorption. Therefore, this investigation can serve as a guide for the design of composite structures. The adsorption of guanine on the ZnO surfaces shows their potential applications in diverse fields in biomedical nanotechnology.

Conflict of Interest

The authors declare no competing financial interest.

ACKNOWLEDGEMENTS

The author (S. Senthilvelan) is highly thankful to UGC, New Delhi for granting a major research project.

REFERENCES

[1] V. Wagner, A. Dullaart, A.K. Bock and A. Zweck, The emerging nanomedicine landscape, *Nat.Biotechnol*., 2006, 24, 1211–1217.

[2] M. Ferrari, Cancer nanotechnology: opportunities and challenges, *Nat. Rev. Cancer*, 2005, 5, 161–171.

[3] R.G. Panchal, Novel therapeutic strategies to selectively kill cancer cells, *Biochem.Pharmacol*., 1998, 55, 247–252.

[4] S. Saha and P. Sarkar, Understanding the interaction of DNA–RNA nucleo bases with different ZnO nanomaterials, *Phys. Chem. Chem. Phys*., 2014, 16, 15355-15366.

[5] A. Nel, T. Xia, L. Mädler and N. Li, Toxic potential of materials at the nanolevel, *Science*, 2006, 311, 622–627.

[6] S. Rakshit and S. Vasudevan, Trap-State Dynamics in Visible-Light-Emitting ZnO:MgO Nanocrystals, *J. Phys. Chem. C*., 2008, 112, 4531–4537.

[7] D. S. Bohle and C. J. Spina, The Relationship of Oxygen Binding and Peroxide Sites and the Fluorescent Properties of Zinc Oxide Semiconductor Nanocrystals, *J. Am. Chem. Soc*., 2007,129, 12380–12381.

[8] H. M. Xiong, Y. Xu, Q. G. Ren and Y. Y. Xia, Stable Aqueous ZnO@Polymer Core–Shell Nanoparticles with Tunable Photoluminescence and Their Application in Cell Imaging, *J. Am. Chem. Soc*., 2008,130, 7522–7523.

[9] H. Wang, D. Wingett and M. H. Engelhard, Fluorescent dye encapsulated ZnO particles with cell-specific toxicity for potential use in biomedical applications, *J. Mater. Sci.: Mater. Med*., 2009, 20, 11–22.

[10] S. Dhobale, T. Thite and S. L. Laware, Zinc oxide nanoparticles as novel alpha-amylase inhibitors, *J. Appl. Phys*., 2008, 104, 094907.

[11] C. Hanley, J. Layne and A. Punnoose, Preferential killing of cancer cells and activated human T cells using zinc oxide nanoparticles, *Nanotechnol*., 2008, 19, 295103–295113.

[12] K.M. Reddy, K. Feris, J. Bell, D.G. Wingett, C. Hanley and A. Punnoose, Selective toxicity of zinc oxide nanoparticles to prokaryotic and eukaryotic systems, *Appl. Phys. Lett*., 2007, 90, 213902-1–3.

[13] A.S. Barnard, One-to-one comparison of sunscreen efficacy, aesthetics and potential nanotoxicity, *Nat. Nanotech.*, 2010, 5, 271 – 274.

[14] J. Musarrat, Q. Saquib, A. Azam and S.A.H. Naqvi, Zinc oxide nanoparticles-induced DNA damage in human lymphocytes, Int. J. Nanopart., 2009, 2, 402–415.

[15] T. Thomas, K. Thomas, N. Sadrieh, N. Savage, P. Adair and R. Bronaugh, Research strategies for safety evaluation of nanomaterials, part VII: evaluating consumer exposure to nanoscale materials, *Toxicol. Sci*., 2006, 91, 14–19.

[16] A.B. Djurisic and Y.H. Leung, Optical properties of ZnO nanostructures, *Small*, 2006, 2, 944–961.

[17] A.V. Kachynski, A.N. Kuzmin, M. Nyk, I. Roy, and P.N. Prasad, Zinc Oxide Nanocrystals for Nonresonant Nonlinear Optical Microscopy in Biology and Medicine, *J. Phys. Chem. C*, 2008, 112, 10721–10724.

[18] S. K. Jain and N. K. Jain, Multiparticulate carriers for sunscreening agents, *Int. J. Cosmet. Sci.*, 2010, 32, 89–98.

[19] K. Schilling, B. Bradford, D. Castelli, E. Dufour, J.F. Nash, W. Pape, S. Schulte, I. Tooley, J. Bosch and F. Schellauf, Human safety review of "nano" titanium dioxide and zinc oxide, *Photochem. Photobiol.Sci.*, 2010, 9, 495-509.

[20] A. K. Jissy and A. Datta, Design and Applications of Noncanonical DNA Base Pairs, *J. Phys. Chem. Lett*., 2014, 5, 154–166.

[21] T. Wang, Y. Hu, L. Zhang, L. Jiang, Z. Chen and N. Y. He, Erythropoietin Nanopariticles: Therapy for CerebralIschemic Injury and Metabolize in Kidney, *Nano Biomed. Eng*., 2010, 2, 31–39.

[22] S. H. Chen, Y. X. Ji, Q. Lian, Y. L. Wen, H. B. Shen and N. Q. Jia, Gold Nanorods Coated with Multilayer Polyelectrolyte as Intracellular delivery Vector of Antisense Oligonucleotides, *Nano Biomed. Eng*., 2010, 2, 15–23.

[23] S. L. Bechara, A. Judson and K. C. Popat, Template synthesized poly(e-caprolactone) nanowire surfaces for neural tissue engineering, *Biomaterials*, 2010, 31, 3492–3501.

[24] Y. Q. Li, Z. Y. Li, X. P. Zhou and P. Yang, Detection of Nano Eu2O3 in Cells and Study of its Biological Effects, *Nano Biomed. Eng*., 2010, 2, 24–30.

[25] V. Shewale, P. Joshi, S. Mukhopadhyay, M. Deshpande, R. Pandey, S. Hussain and S.P. Karna, First-principles study of nanoparticle-biomolecular interactions: Anchoring of a $(ZnO)_{12}$ cluster on nucleobases, *J. Phys. Chem. C*, 2011, 115, 10426–10430.

[26] A. Jain, V. Kumar and Y. Kawazoe, Ring structures of small ZnO clusters, Comput. *Mater. Sci.*, 2006, 36, 258–262.

[27] R.P. Lopes, M. Paula, M. Marques, R. Valero, J. Tomkinson and L.A.E. Batista de Carvalho, Guanine: A combined study using vibrational spectroscopy and theoretical methods, *Spectrosc. Int. J.*, 2012, 27, 273–292.

[28] W. Liang, H. Li, X. Hu and S. Han, Systematic theoretical investigations on all of the tautomers of guanine: from both dynamics and thermodynamics viewpoint, *Chem. Phys*., 2006, 328, 93–102.

[29] M. Y. Choi and R. E. Miller, Four tautomers of isolated guanine from infrared laser spectroscopy in helium nanodroplets, *J. Am. Chem. Soc*., 2006,128, 7320– 7328.

[30] M.J. Frisch, G.W. Trucks, H.B. Schlegel, G.E. Scuseria, M.A. Robb, J.R. Cheeseman, J.A.J. Montgomery and J.A.J. Vreven, Gaussian 03, Revision D.01; Gaussian, Inc.: Wallingford, CT, USA, 2004.

[31] N.M. O'Boyle, A.L. Tenderholt and K.M. Lagner, cclib: A library for package-independent computational chemistry algorithms, *J. Comput. Chem*., 2008, 29, 839–845.

[32] M.T. Baei, DFT Study of CO_2 Adsorption on the $Zn_{12}O_{12}$ Nano-cage, *Bull. Korean Chem. Soc*., 2013, 34, 3722-3726.

[33]C.E. Szakacs, E.F.S. Merschrod and K.M. Poduska, Structural Features That Stabilize ZnO Clusters: An Electronic Structure Approach, *Computation*, 2013, 1, 16-26.

[34] H.P. Chen, J.N. Ding, N.Y. Yuan, X.Q. Wang, C.L. Chen and D. Weng, First-principle study of interaction of H_2 and H_2O molecules with $(ZnO)_{n(n=3-6)}$ ring clusters, *Prog. Nat. Sci*., 2010, 20, 30−37.

[35] S.J. Grabowski, W.A. Sokalski, E. Dyguda and J. Leszczynski, Quantitative Classification of Covalent and Noncovalent H-bonds, *J. Phys. Chem. B*, 2006, 110, 6444–6446.

[36] A. Jayaprakash, V. Arjunan, S.P. Jose and S. Mohan, Vibrational and electronic investigations, thermodynamic parameters, HOMO and LUMO analysis on crotonaldehyde by ab initio and DFT methods, *Spectrochim. Acta*, 2011, 83, 411– 419.

[37] B. Wang, S. Nagase, J. Zhao and G. Wang, Structural grouth sequences and electronic properties of Zinc oxide clusters $(ZnO)_n$ (n=2-18), *J. Phys. Chem. C*, 2007, 111, 4956-4963.

[38] C. Arunagiri, A. Subashini, M. Saranya, P.T. Muthiah, Molecular Structure, Optimized Geometry, HOMO LUMO Energy and Mulliken Charges of a New Schiff Base 2-(Naphthalen-2-yliminomethyl) Phenol by ab Initio and Density Functional Theory Calculations, *Ind. J. Appl. Res.*, 2013, 3, 78-81.

[39] D. C. Aggarwal, SHI induced modification of ZnO thin film: Optical and structural studies, *Nucl. Instrum. Methods Phys. Res. B*, 2006, 244, 136–140.

[40] R. Wahab, Y.S. Kim, I.H. Hwang, H.S. Shin, A non-aqueous synthesis, characterization of zinc oxide nanoparticles and their interaction with DNA, *Synth. Met.*, 2009, 159, 2443–2452.

[41] I.M. Deneva, Infrared spectroscopy investigation of metallic nanoparticles based on copper, cobalt, and nickel synthesized through borohydride reduction method, *J. University Chem. Technol. Metall.*, 2010, 45, 351-378.

[42] A.R.T. Benavides, M. Tlahuextl, H. Tlahuext, C.G. Vidal, Synthesis of Zn compounds derived from 1H-benzimidazol-2-ylmethanamine, Issue in Honor of Prof Rosalinda Contreras Theurel, ARKIVOC 2008, 172-186.

[43] D.R. Tackley, G. Dent and W.E. Smith, IR and Raman assignments for zinc phthalocyanine from DFT calculations, Phys. Chem. Chem. Phys., 2000, 2, 3949-3955

[44] H.M. Cheng, K.F. Lin, H.C. Hsu, C.J. Lin, L.J. Lin and W.F. Hsieh, Enhanced resonant Raman scattering and electron-phonon coupling from self-assembled secondary ZnO nanoparticles, *J. Phys. Chem. B*, 2005, 109, 18385-18390.

[45] N. Ashkenov, B.N. Mbenkum, C. Bundesmann, V. Riede, M. Lorenz, D. Spemann, E.M. Kaidashev, A. Kasic, M. Shubert and M. Grundmann, Infrared dielectric functions and phonon modes of high-quality ZnO films, *J. Appl. Phys*., 2003,93, 126–133.

[46] Y.P. Du, Y.W. Zhang, L.D. Sun and C.H. Yan, Efficient energy transfer in mono disperse Eu-doped ZnO nanocrystals synthesized from metal acetylacetonates in high-boiling solvents, *J. Phys. Chem. C*, 2008,112, 12234–12241.

[47] N.P.G. Roeges, A Guide to Complete Interpretation of Infrared Spectra of Organic Structures, Wiley, NewYork, 1994.

[48] B. Giese and D. McNaughton, Density functional theoretical (DFT) and surface-enhanced Raman spectroscopic study of guanine and its alkylated derivatives: part 1. DFT calculations on neutral, protonated and deprotonated guanine, *Phys. Chem. Chem. Phys*., 2002, 4, 5161–5170.

[49] R. Santamaria, E. Charro, A. Zacarıas and M. Castro, Vibrational spectra of nucleic acid basesand their Watson-Crick pair complexes, *J. Comput. Chem*., 1999, 20, 511–530.

[50] B. Pergolese, A. Bonifacio and A. Bigotto, SERS studies of the adsorption of guanine derivatives on gold colloidal nanoparticles, *Phys .Chem. Chem. Phys*., 2005, 7, 3610–361.

Captions for Figures and Table

Fig. 1. Optimized structure of ZnO clusters (a) Zn_2O_2, (b) Zn_3O_3, (c) Zn_4O_4 (R) and (d) Zn_4O_4 (W)

Fig. 2. Density of state plots for ZnO clusters (a) Zn_2O_2, (b) Zn_3O_3, (c) Zn_4O_4 (R) and (d) Zn_4O_4 (W)

Fig. 3. Models for four optimized structure of G/ZnO clusters (a) G/Zn_2O_2, (b) G/Zn_3O_3, (c) G/Zn_4O_4 (R) and (d) G/Zn_4O_4 (W)

Fig. 4. (a) Optimized structure and (b) Density of state plot for guanine

Fig. 5. Density of state plots for G/ZnO clusters (a) G/Zn_2O_2, (b) G/Zn_3O_3, (c) G/Zn_4O_4 (R) and (d) G/Zn_4O_4 (W)

Fig. 6. Electron distribution plot for HOMO (a) G/Zn_2O_2, (b) G/Zn_3O_3, (c) G/Zn_4O_4 (R), (d) G/Zn_4O_4 (W) and electron distribution plot for LUMO (e) G/Zn_2O_2, (f) G/Zn_3O_3, (g) G/Zn_4O_4 (R), (h) G/Zn_4O_4 (W).

Fig. 7. Models for three optimized structure of G/Zn_2O_2 clusters (a) –N2 site, (b) –NH_2 site and (c) –O site.

Fig. 8. FT-IR spectra of (a) ZnO nanoparticle, (b) G/ZnO composite and (c) guanine molecule

Fig. 9. Simulated IR spectra for ZnO and G/ZnO clusters

Fig. 10. FT-RAMAN spectra of (a) ZnO nanoparticle, (b) G/ZnO composite and (c) guanine molecule

Fig. 11. Simulated RAMAN spectra for ZnO and G/ZnO clusters

Fig. 12. SEM images of (a) ZnO nanoparticles and (b) G/ZnO composite, EDX analysis of (c) ZnO nanoparticles and (d) G/ZnO composite.

Fig. 13. (a) FE-SEM image of ZnO nanoparticles and UV-visible spectra of (b) ZnO nanoparticles, (c) Guanine molecule and (d) G/ZnO composite

Table. 1. The calculated HOMO energies (E_{HOMO}), LUMO energies (E_{LUMO}), HOMO–LUMO energy gab (E_g), distance of Zn–N (Å), binding energies (E_B) and scaled energies (E_S) by using B3LYP/LanL2DZ.

Table. 2. Mulliken atomic charges of ZnO and G/ZnO clusters at B3LYP/LanL2DZ basis set

Table. 3. The calculated HOMO-LUMO energy gap (E_g) of ZnO and G/ZnO clusters by using B3LYP/6-31G, B3LYP/6-311G, MP2/6-31G and MP2/LanL2DZ basis set.

“FIGURES and TABLE

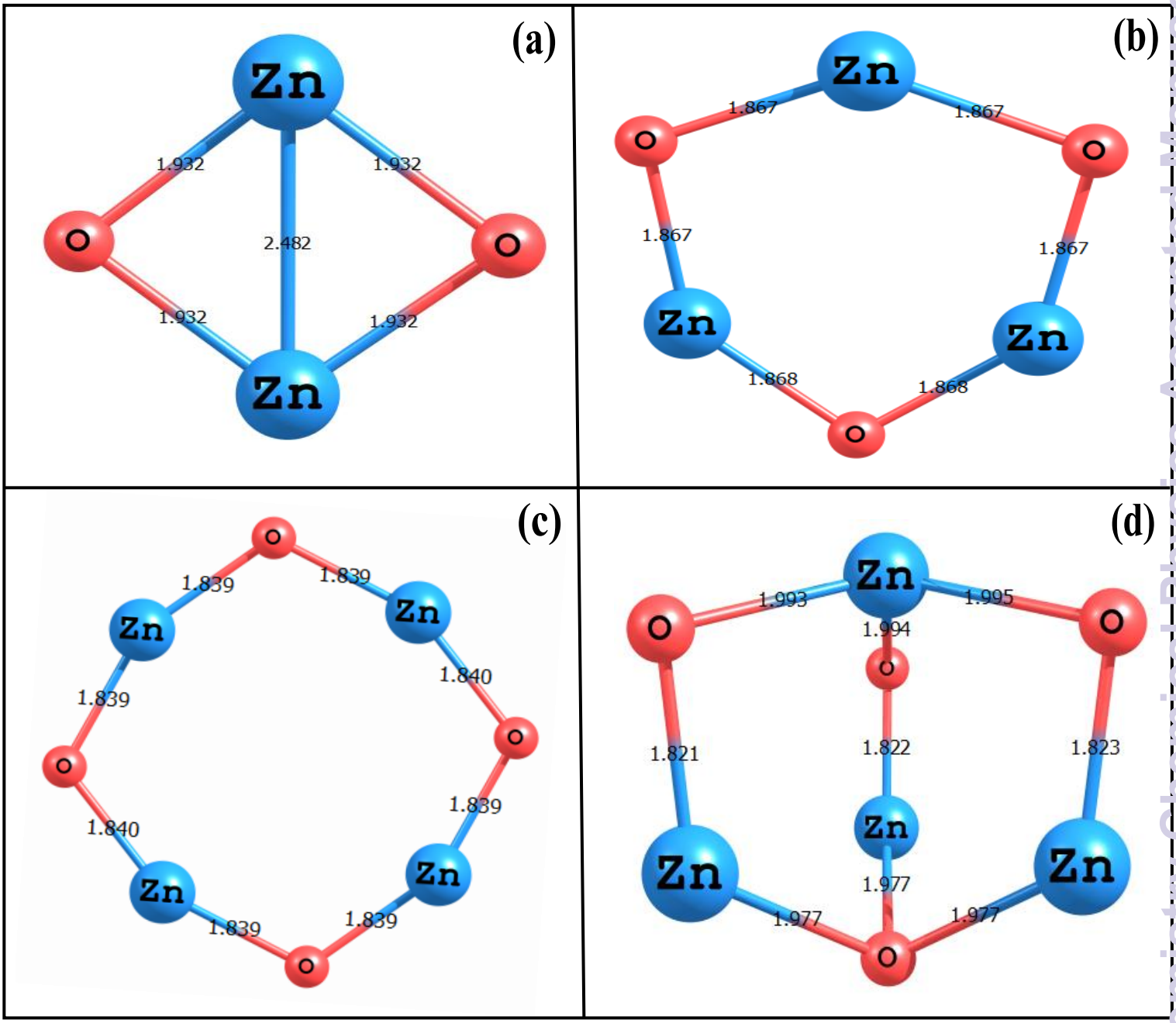

Fig. 1. Optimized structure of ZnO clusters (a) Zn_2O_2, (b) Zn_3O_3, (c) Zn_4O_4 (R) and (d) Zn_4O_4 (W)

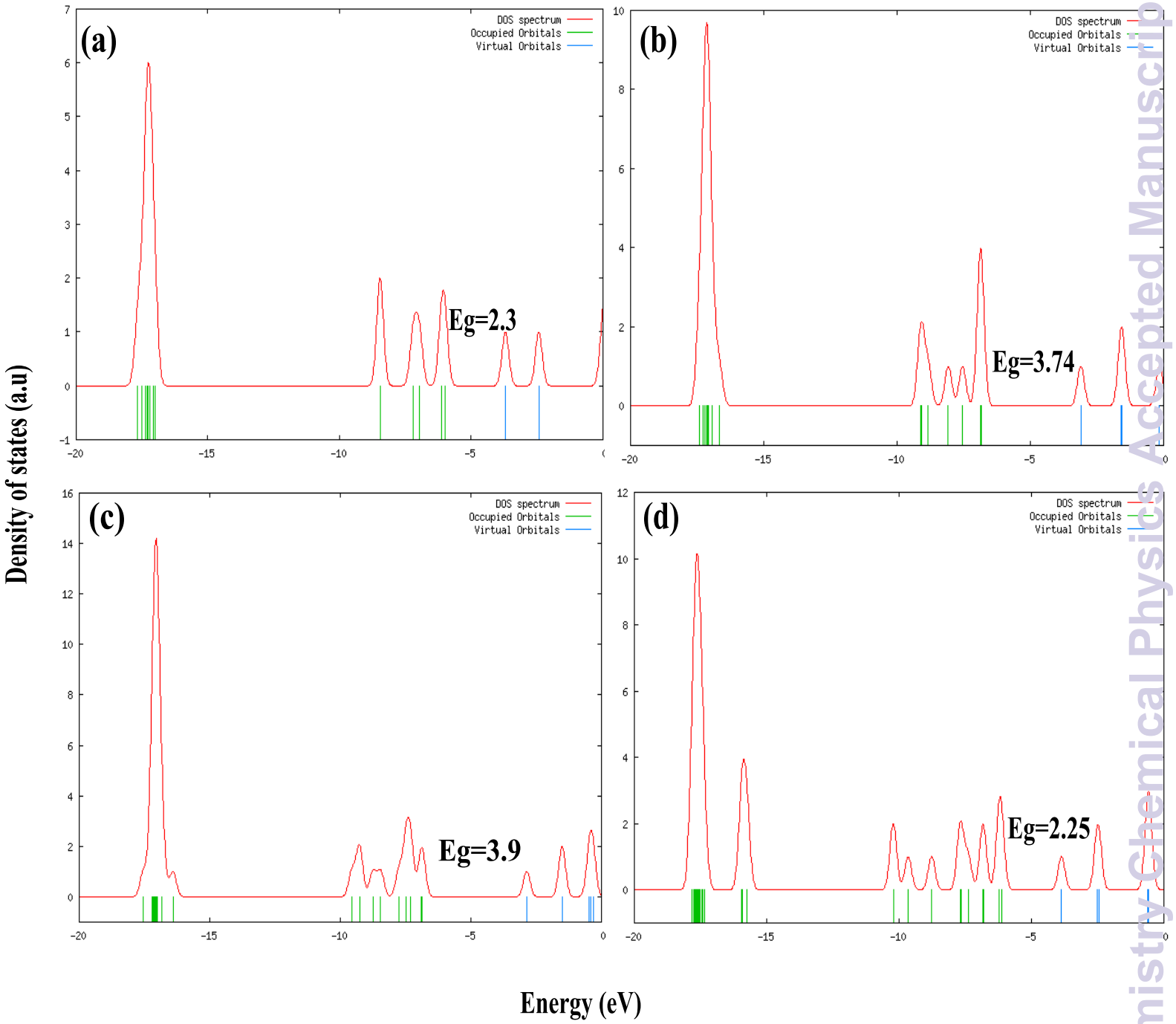

Fig. 2. Density of state plots for ZnO clusters (a) Zn_2O_2, (b) Zn_3O_3, (c) Zn_4O_4 (R) and (d) Zn_4O_4 (W)

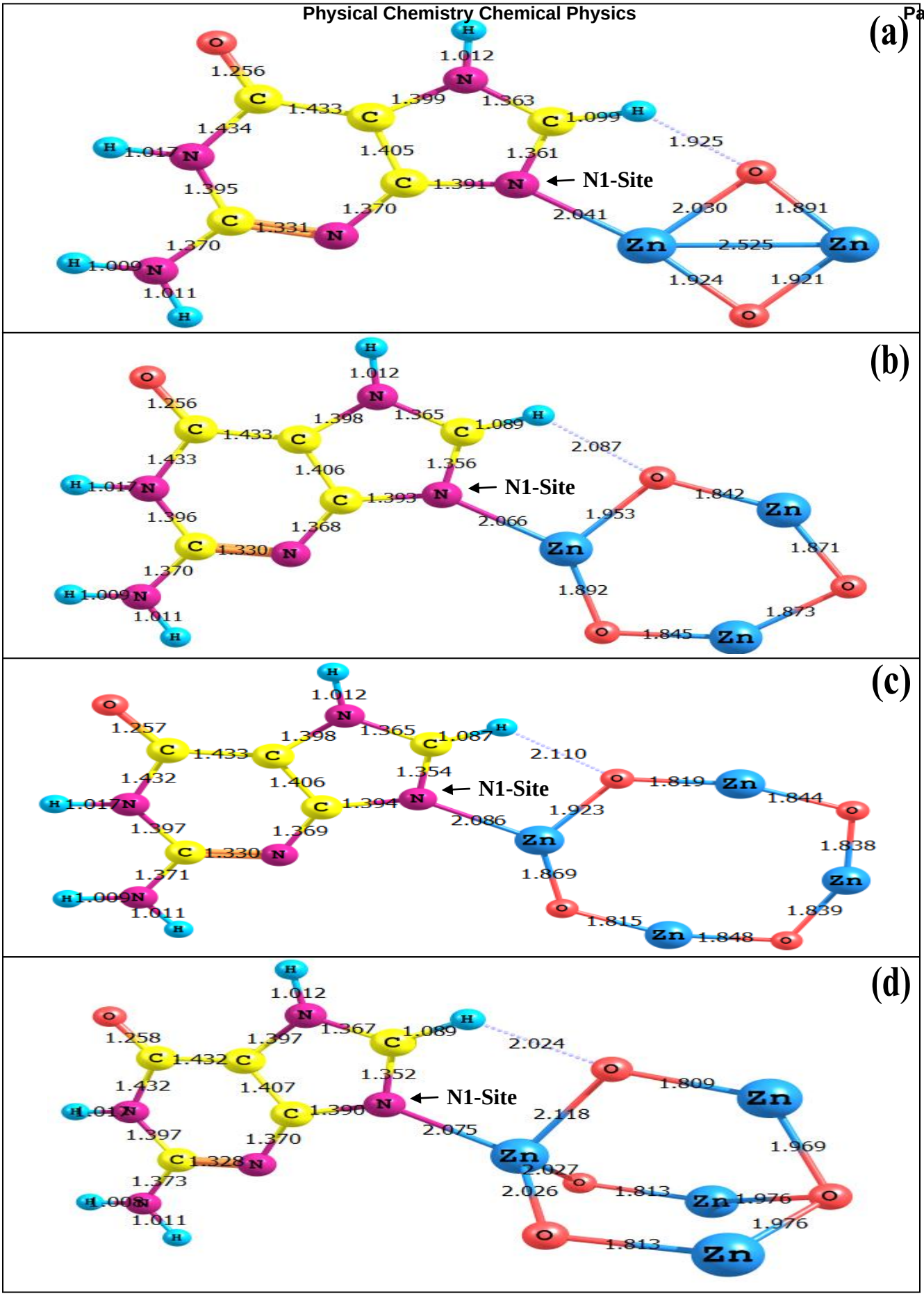

Fig. 3. Models for four optimized structure of G/ZnO clusters (a) G/Zn_2O_2, (b) G/Zn_3O_3, (c) G/Zn_4O_4 (R) and (d) G/Zn_4O_4 (W)

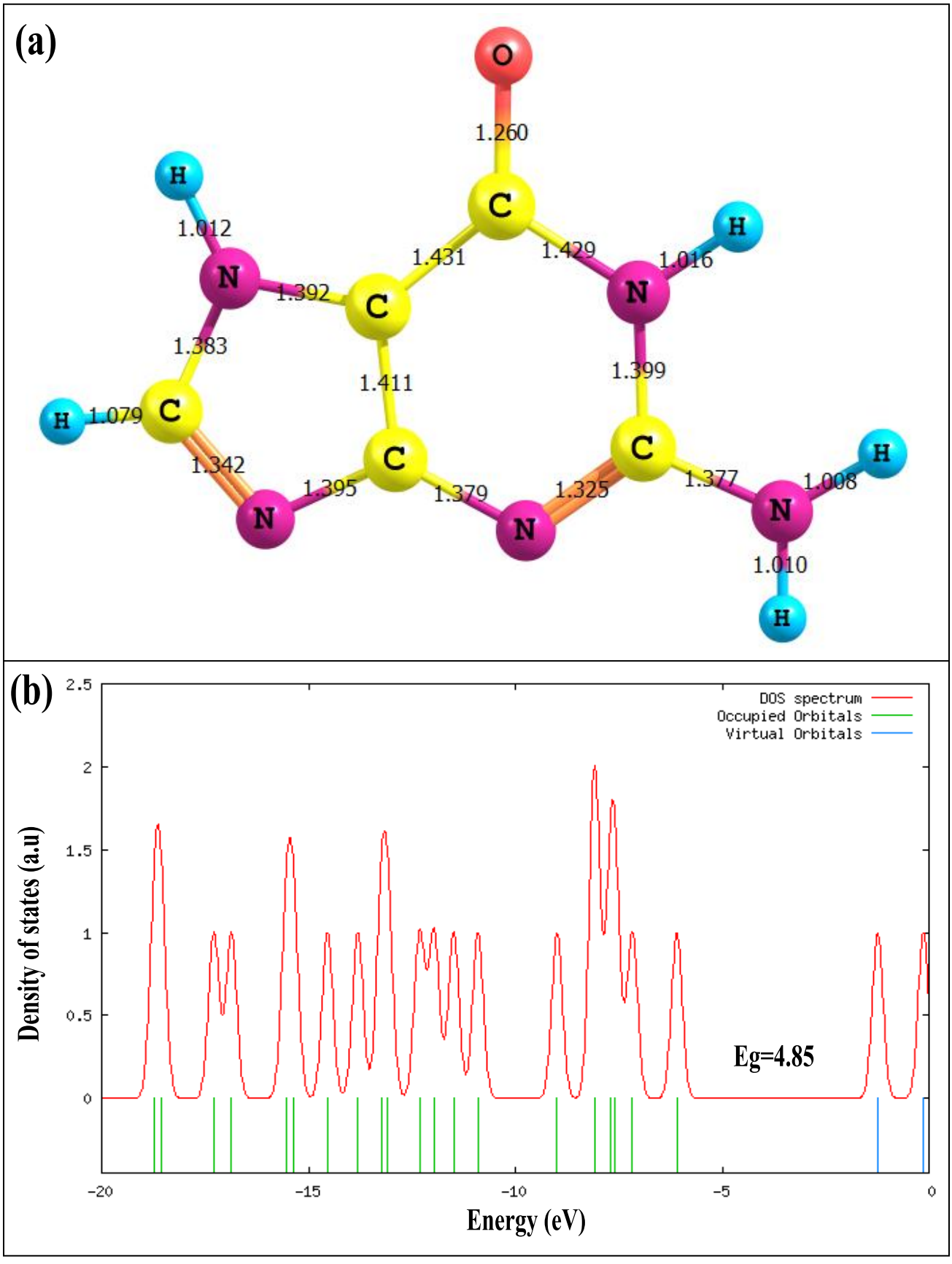

Fig. 4. (a) Optimized structure and (b) Density of state plot for guanine

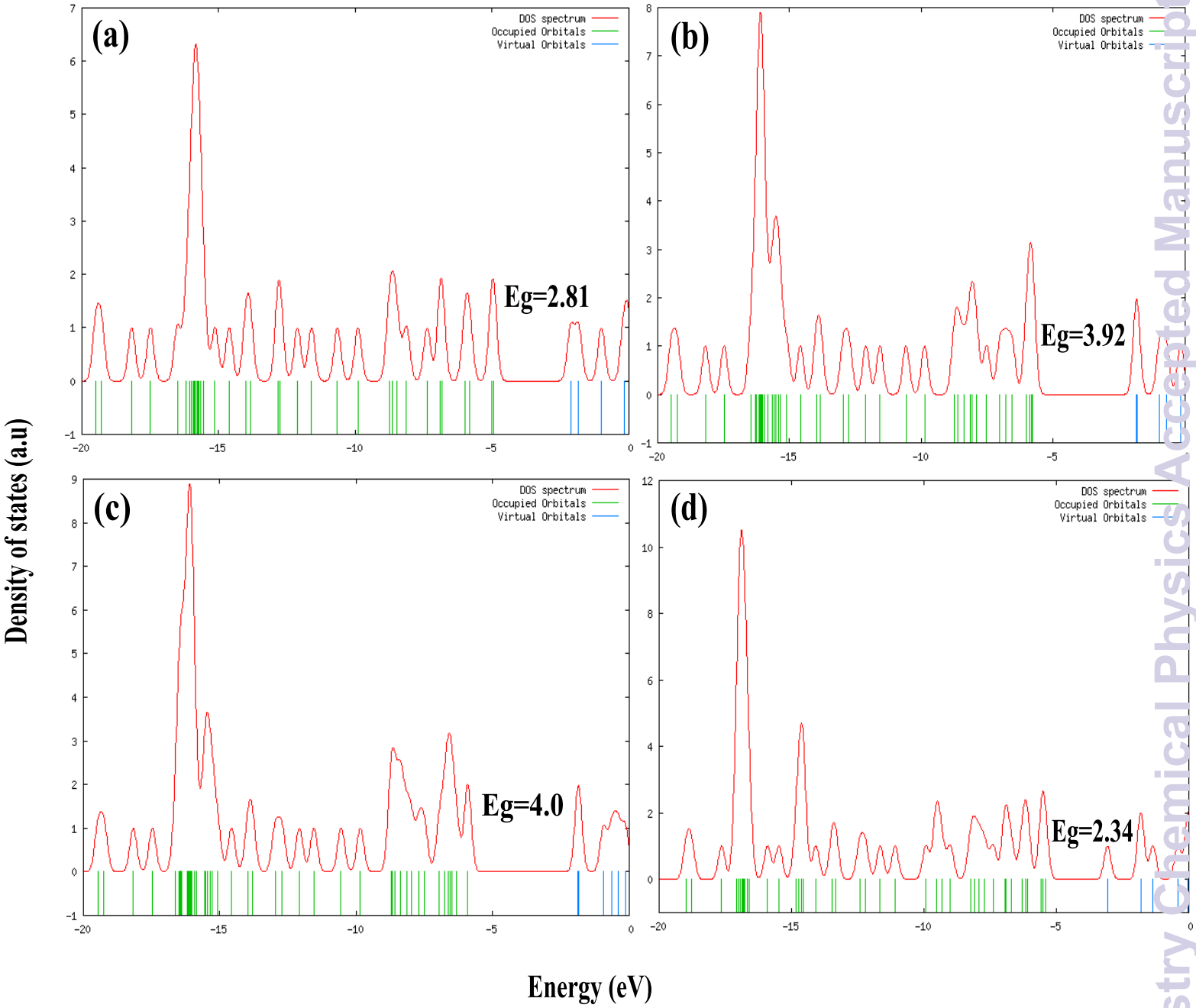

Fig. 5. Density of state plots for G/ZnO clusters (a) G/Zn_2O_2, (b) G/Zn_3O_3, (c) G/Zn_4O_4 (R) and (d) G/Zn_4O_4 (W)

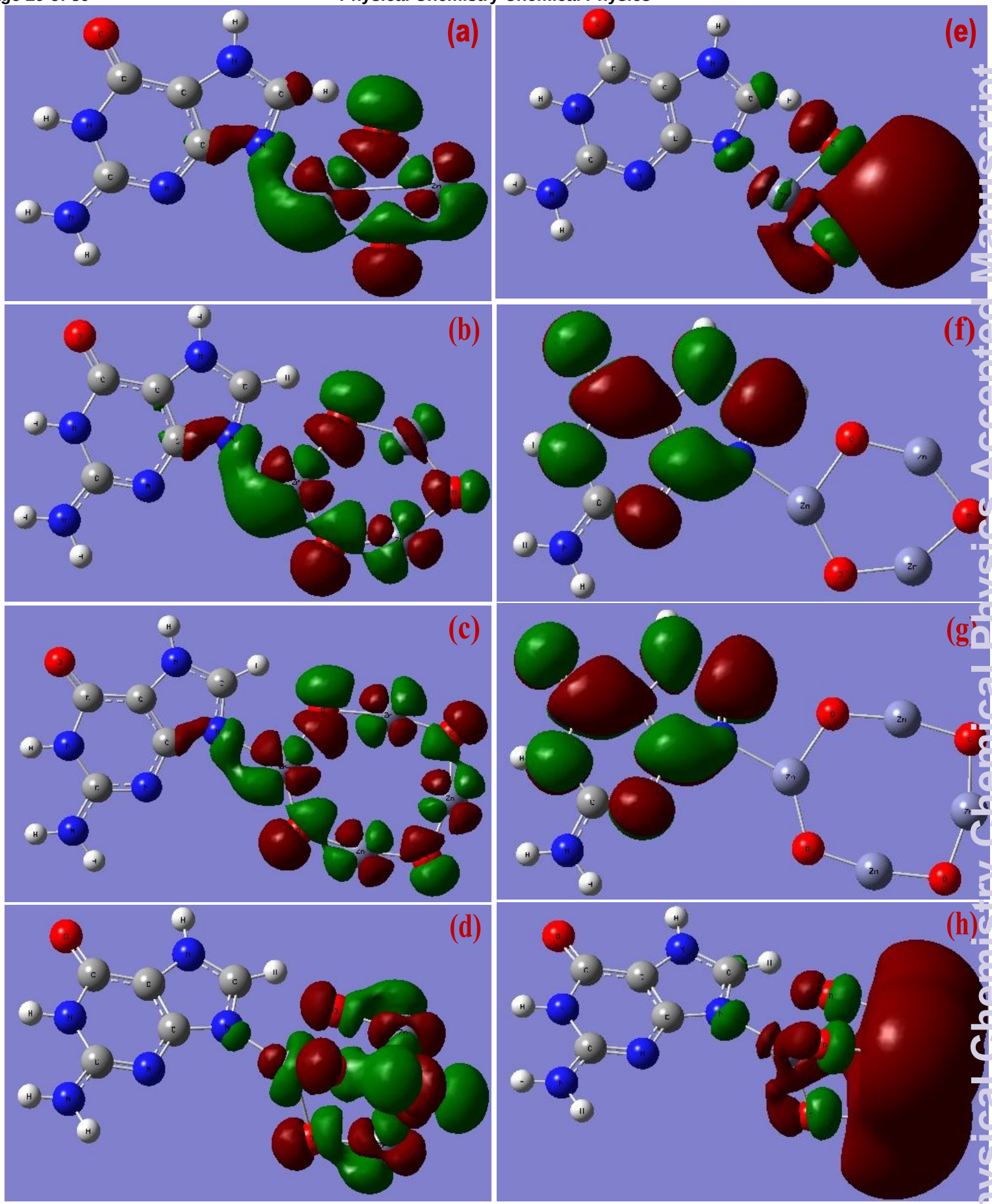

Fig. 6. Electron distribution plot for HOMO (a) G/Zn_2O_2, (b) G/Zn_3O_3, (c) G/Zn_4O_4 (R), (d) G/Zn_4O_4 (W) and electron distribution plot for LUMO (e) G/Zn_2O_2, (f) G/Zn_3O_3, (g) G/Zn_4O_4 (R), (h) G/Zn_4O_4(W).

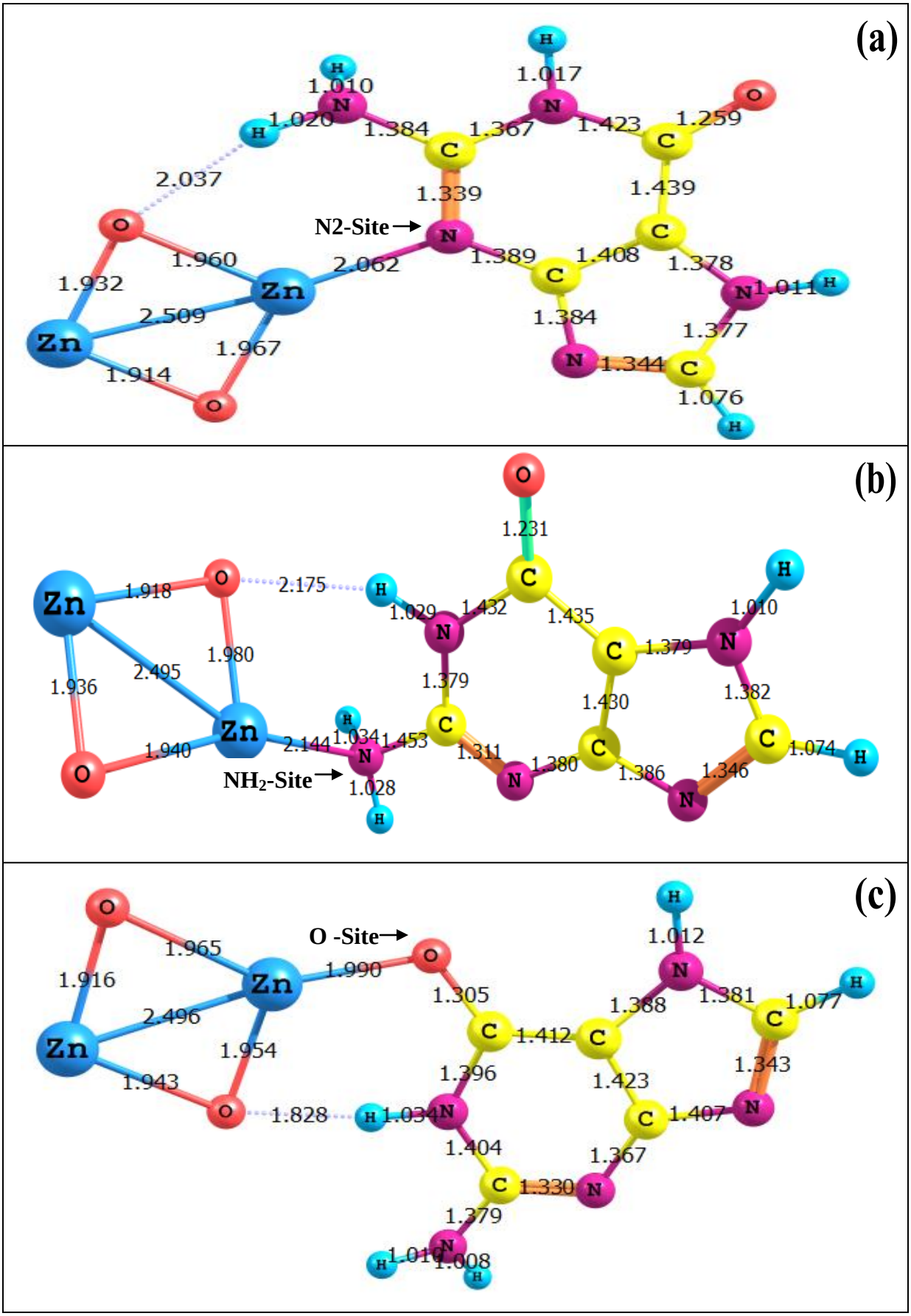

Fig. 7. Models for three optimized structure of G/Zn_2O_2 clusters (a) –N2 site, (b) $–NH_2$ site and (c) –O site.

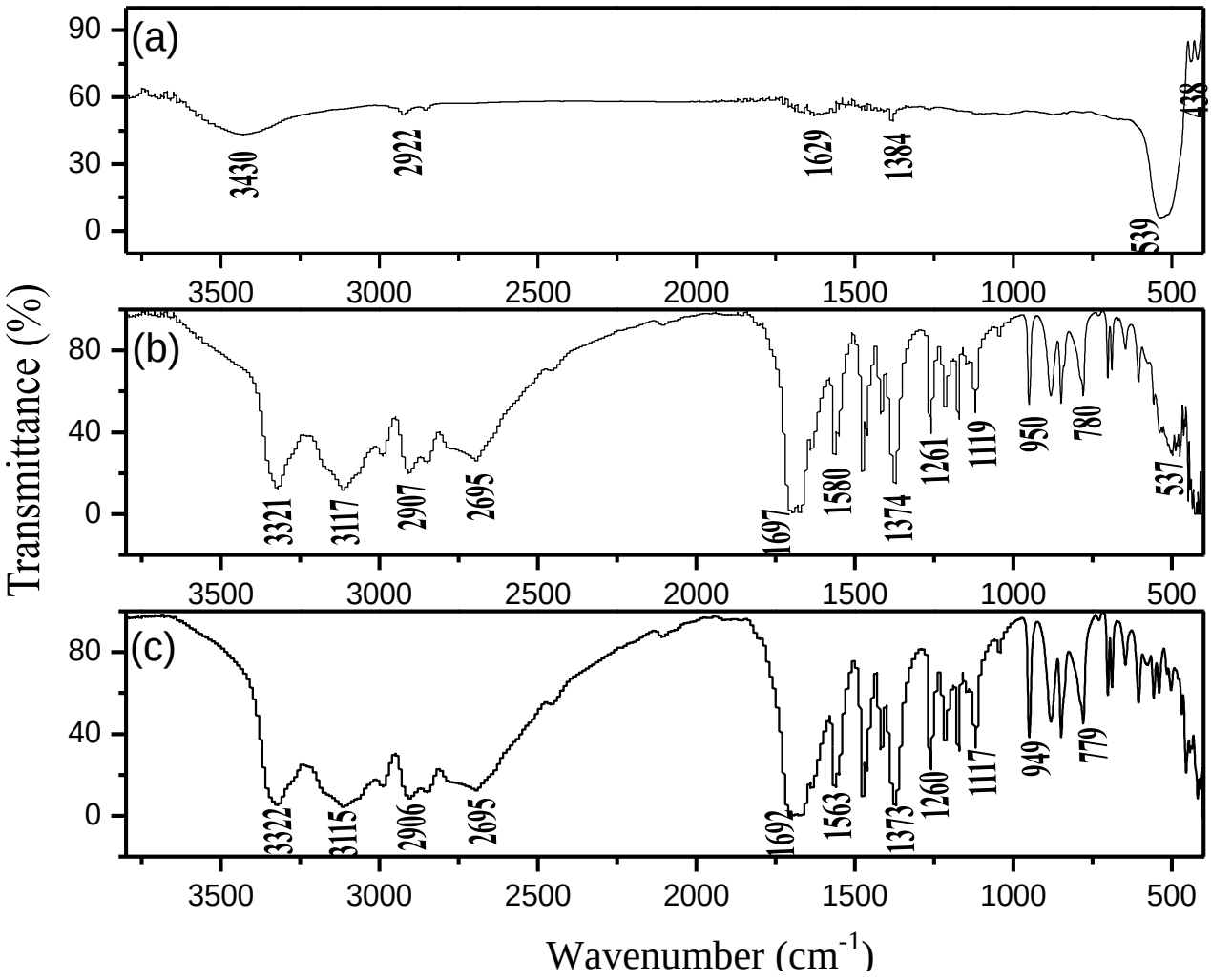

Fig. 8. FT-IR spectra of (a) ZnO nanoparticle, (b) G/ZnO composite and (c) guanine molecule

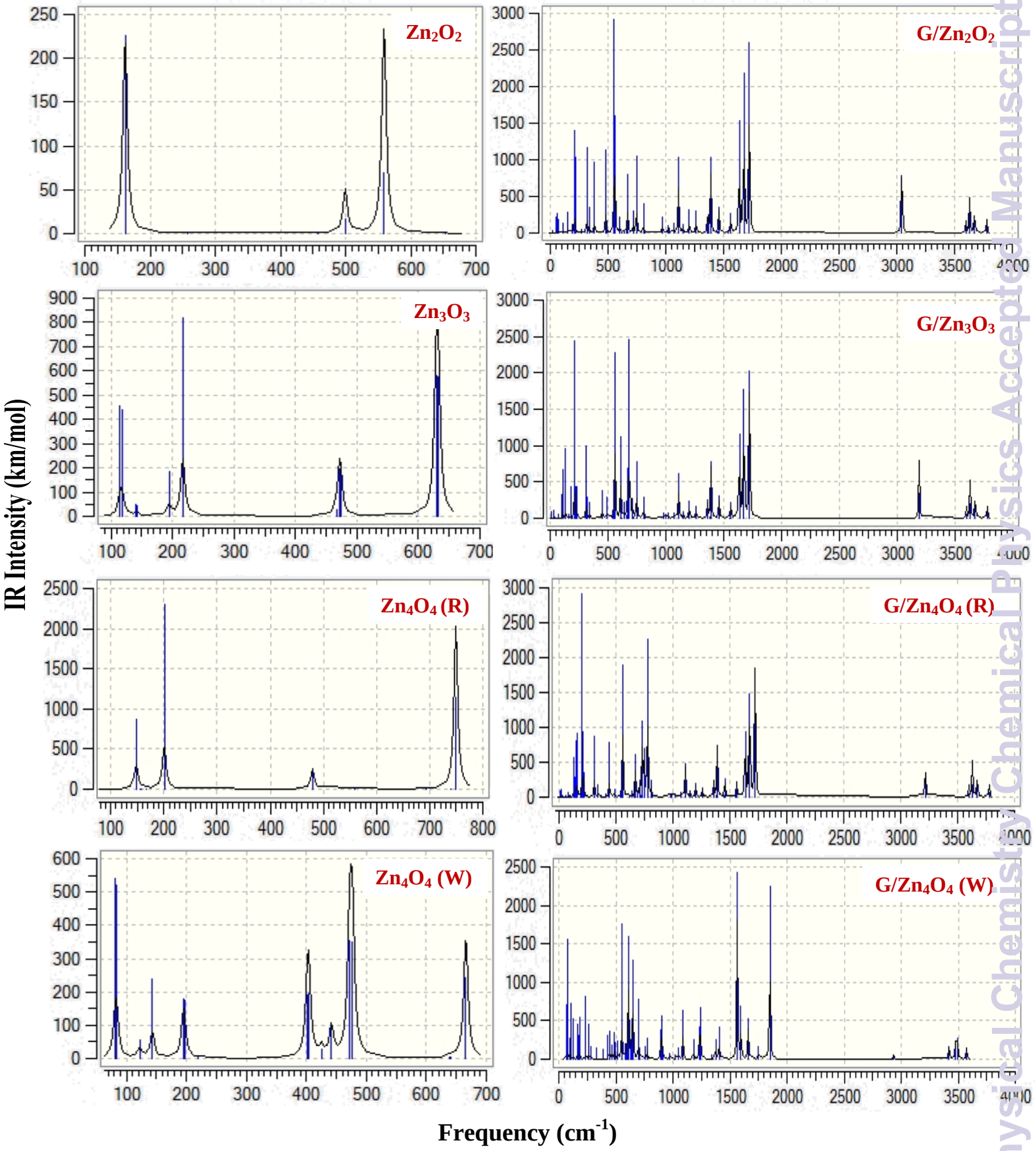

Fig. 9. Simulated IR spectra for ZnO and G/ZnO clusters

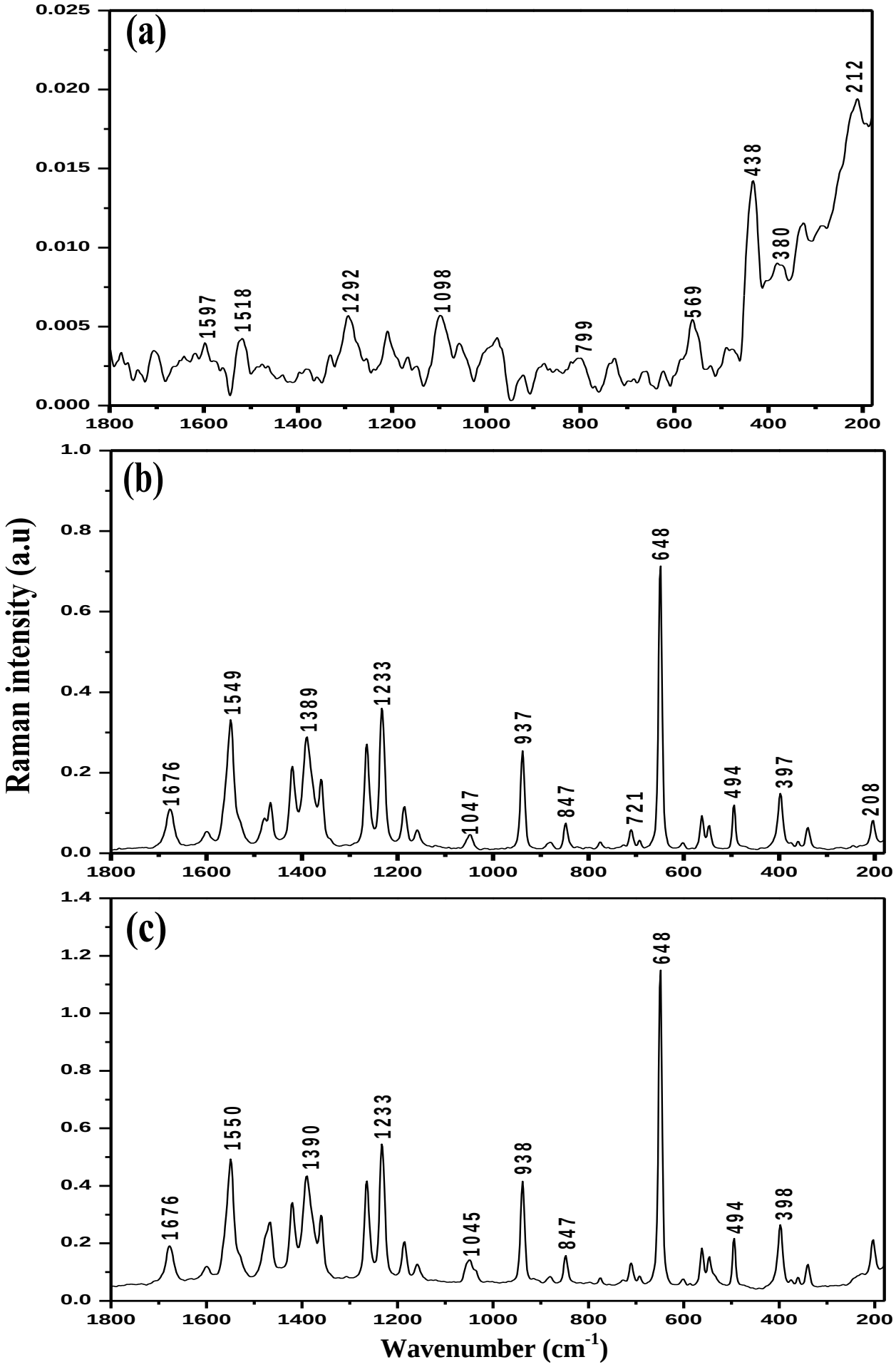

Fig. 10. FT-RAMAN spectra of (a) ZnO nanoparticle, (b) G/ZnO composite and (c) guanine molecule

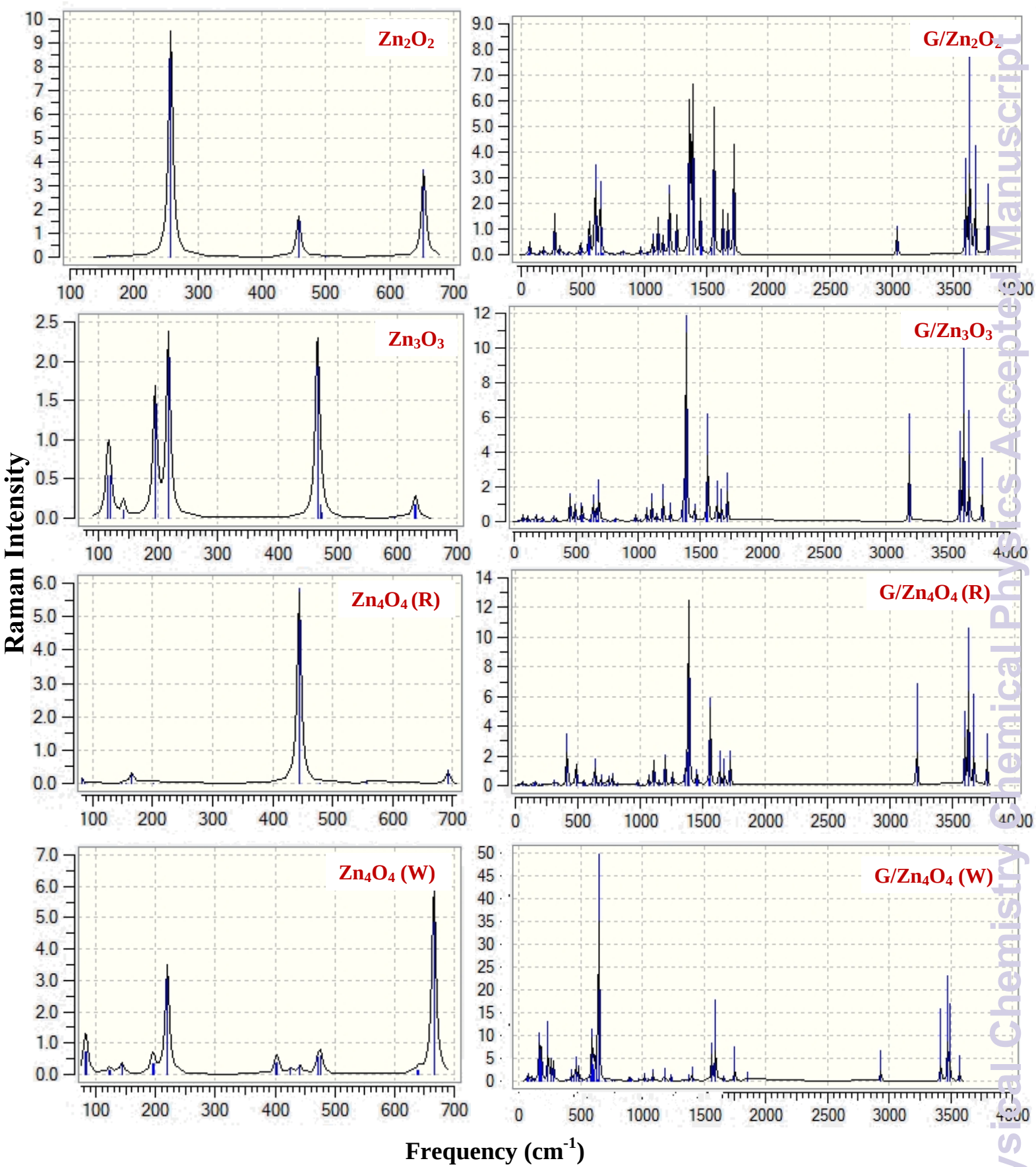

Fig. 11. Simulated RAMAN spectra for ZnO and G/ZnO clusters

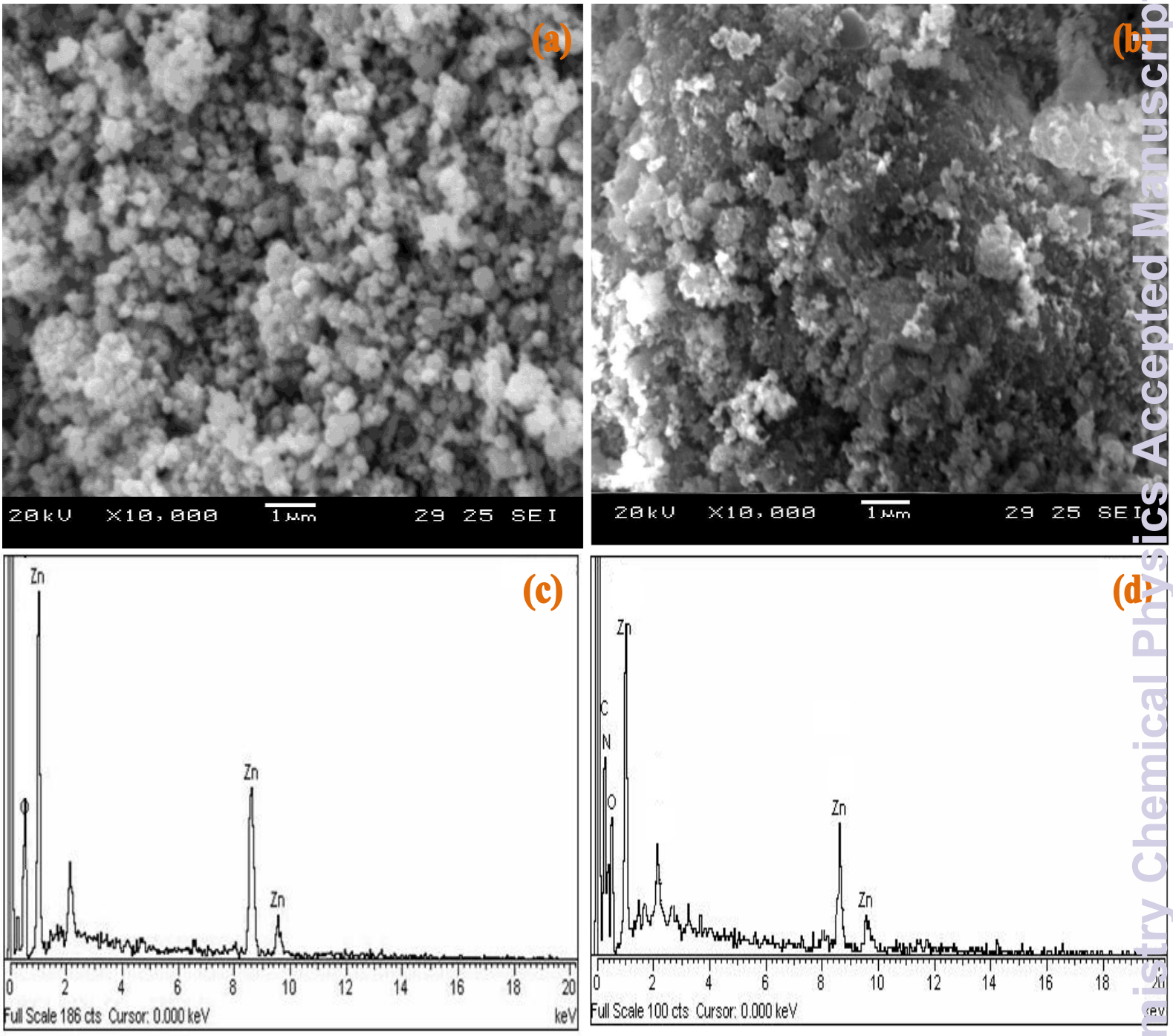

Fig. 12. SEM images of (a) ZnO nanoparticles and (b) G/ZnO composite, EDX analysis of (c) ZnO nanoparticles and (d) G/ZnO composite.

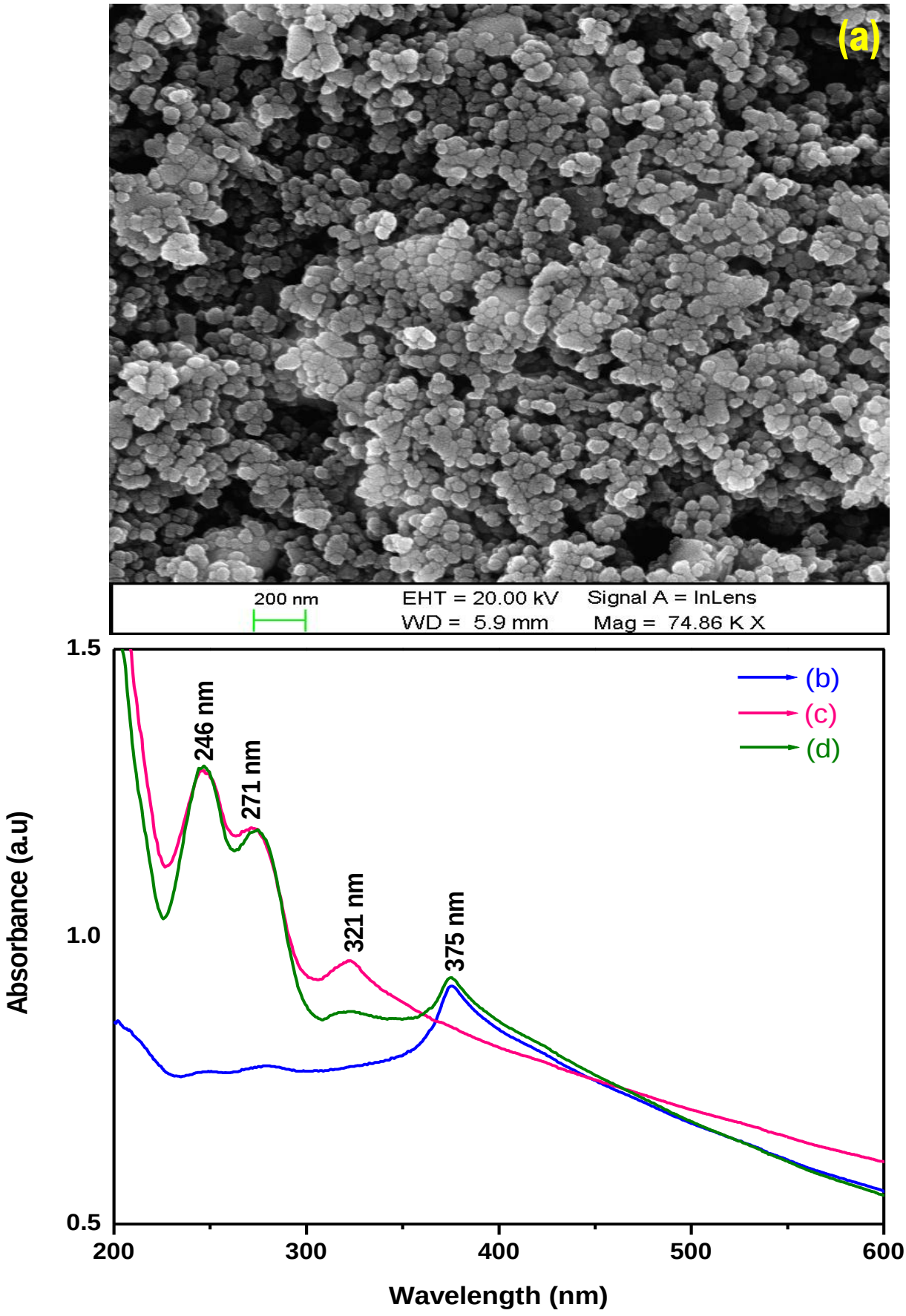

Fig. 13. (a) FE-SEM image of ZnO nanoparticles and UV-visible spectra of (b) ZnO nanoparticles, (c) Guanine molecule and (d) G/ZnO composite

Table. 1. The calculated HOMO energies (E_{HOMO}), LUMO energies (E_{LUMO}), HOMO–LUMO energy gab (E_g), distance of Zn–N (Å), binding energies (E_B) and scaled energies (E_S) by using B3LYP/LanL2DZ.

Structure	E_{HOMO} (eV)	E_{LUMO} (eV)	E_g (eV)	Distance of Zn–N (Å)	E_B (eV)	E_S (eV)
1. Zn_2O_2	- 6.0	- 3.70	2.30	–	6.12	- 1915.52
2. Zn_3O_3	- 6.85	- 3.11	3.74	–	7.34	- 1916.13
3. Zn_4O_4 (R)	- 6.84	- 2.85	3.90	–	7.75	- 1916.33
4. Zn_4O_4 (W)	- 6.12	- 3.87	2.25	–	7.21	- 1916.07
5. G/Zn_2O_2	- 4.94	- 2.13	2.81	2.04	2.17	–
6. G/Zn_3O_3	- 5.78	- 1.86	3.92	2.06	1.90	–
7. G/Zn_4O_4(R)	- 5.91	- 1.87	4.01	2.08	1.62	–
8. G/Zn_4O_4 (W)	- 5.41	- 3.07	2.34	2.07	1.63	–
9. Guanine	- 6.09	- 1.24	4.85	–	–	–

Table. 2. Mulliken atomic charges of ZnO and G/ZnO clusters at B3LYP/LanL2DZ basis set

Atoms (Zn_2O_2)	Atomic charges	Atoms (Zn_3O_3)	Atomic charges	Atoms [Zn_4O_4(W)]	Atomic charges
Zn_1	0.831	Zn_1	0.888	Zn_1	0.945
O_2	-0.831	O_2	-0.888	O_2	-0.945
O_3	0.831	O_3	-0.889	O_3	-0.829
Zn_4	-0.831	O_4	-0.887	Zn_4	0.830
		Zn_5	0.887	O_5	-0.829
		Zn_6	0.889	O_6	-0.830
				Zn_7	0.830
				Zn_8	0.828
Atoms(G/Zn_2O_2)	Atomic charges	Atoms(G/Zn_3O_3)	Atomic charges	Atoms[G/Zn_4O_4(W)]	Atomic charges
N_1	-0.355	N_1	-0.358	N_1	-0.356
C_2	-0.082	C_2	-0.075	C_2	-0.087
N_3	-0.395	N_3	-0.365	N_3	-0.346
C_4	0.086	C_4	0.089	C_4	0.105
N_5	-0.052	N_5	-0.039	N_5	-0.037
C_6	0.201	C_6	0.195	C_6	0.191
N_7	-0.621	N_7	-0.621	N_7	-0.625
N_8	-0.411	N_8	-0.412	N_8	-0.409
C_9	0.152	C_9	0.149	C_9	0.145
O_{10}	-0.284	O_{10}	-0.285	O_{10}	-0.295
C_{11}	0.121	C_{11}	0.118	C_{11}	0.117
Zn_{12}	0.913	Zn_{12}	0.955	Zn_{12}	0.979
O_{13}	-0.843	O_{13}	-0.885	O_{13}	-0.941
O_{14}	-0.929	O_{14}	-0.929	O_{14}	-0.818
Zn_{15}	0.727	O_{15}	-0.958	Zn_{15}	0.782
H_{16}	0.354	Zn_{16}	0.823	O_{16}	- 0.818
H_{17}	0.389	Zn_{17}	0.816	O_{17}	- 0.879
H_{18}	0.362	H_{18}	0.351	Zn_{18}	0.788
H_{19}	0.325	H_{19}	0.368	Zn_{19}	0.783
H_{20}	0.341	H_{20}	0.365	H_{20}	0.344
		H_{21}	0.324	H_{21}	0.361
		H_{22}	0.341	H_{22}	0.362
				H_{23}	0.319
				H_{24}	0.335

Table. 3. The calculated HOMO-LUMO energy gap (E_g) of ZnO and G/ZnO clusters by using B3LYP/6-31G, B3LYP/6-311G, MP2/6-31G and MP2/LanL2DZ basis set.

Structure	B3LYP/6-31G	B3LYP/6-311G	MP2/6-31G	MP2/LanL2DZ
	E_g (eV)	E_g (eV)	E_g (eV)	E_g (eV)
1. Zn_2O_2	2.47	2.56	8.80	7.97
2. Zn_3O_3	4.23	3.78	10.59	9.26
3. Zn_4O_4 (R)	4.34	3.79	10.31	9.96
4. Zn_4O_4 (W)	2.68	2.55	9.18	8.25
4. G/Zn_2O_2	3.10	2.88	6.4	6.76
5. G/Zn_3O_3	4.20	3.48	7.79	6.78
6. G/Zn_4O_4 (R)	4.21	3.50	8.53	7.74
8. G/Zn_4O_4 (W)	2.82	2.52	7.57	7.61